J Solid State Electrochem (2012) 16:569–578
DOI 10.1007/s10008-011-1381-0

ORIGINAL PAPER

Blocking properties of gold electrodes modified with 4-nitrophenyl and 4-decylphenyl groups

Marko Kullapere · Margus Marandi · Leonard Matisen · Fakhradin Mirkhalaf · Adriana E. Carvalho · Gilberto Maia · Väino Sammelselg · Kaido Tammeveski

Received: 22 November 2010 / Revised: 12 March 2011 / Accepted: 14 March 2011 / Published online: 20 April 2011

Abstract The electrochemical properties of Au electrodes grafted with 4-nitrophenyl and 4-decylphenyl groups have been studied. The electrografting of gold electrode surface with aryl groups was carried out by electroreduction of the corresponding diazonium salts in acetonitrile. The nitrophenyl film growth on gold was examined by atomic force microscopy, electrochemical quartz crystal microbalance and X-ray photoelectron spectroscopy. These measurements showed that a multilayer film of nitrophenyl groups was formed. Cyclic voltammetry was used to study the blocking properties of aryl-modified gold electrodes towards the $Fe(CN)_6^{3-/4-}$ redox system. The reduction of oxygen was strongly suppressed on these electrodes as evidenced by the rotating disc electrode results.

Keywords Electrochemical grafting · Diazonium salts · Gold electrode · Oxygen reduction · Hexacyanoferrate

M. Kullapere · M. Marandi · V. Sammelselg · K. Tammeveski (✉)
Institute of Chemistry, University of Tartu,
Ravila 14a,
50411, Tartu, Estonia
e-mail: kaido@chem.ut.ee

M. Marandi · L. Matisen · V. Sammelselg
Institute of Physics, University of Tartu,
Riia 142,
51014, Tartu, Estonia

F. Mirkhalaf
Sonochemistry Centre, Coventry University,
Coventry CV1 5FB, UK

A. E. Carvalho · G. Maia
Department of Chemistry, UFMS,
CP 549,
Campo Grande, MS 79070-900, Brazil

Introduction

The electrochemical grafting of aryl groups to conductive surfaces via reduction of diazonium compounds has become a widely used method in surface modification [1–10]. Although the method is mostly employed for the modification of carbon materials [1–4], it has also been successfully used for the modification of metal electrode surfaces [11–25]. The electrografting of gold electrodes with aryl groups was first demonstrated by Ahlberg et al. [26], however, the advantages of diazonium reduction for the modification of Au surfaces have only recently attracted a great deal of attention [8, 11, 19, 27–54]. The first step in the modification of electrode surfaces via electroreduction of aryldiazonium cations is the formation of an aryl radical which appears to attack the substrate to form a covalent bond [2]. The mechanism of attachment of aryl groups to gold is not entirely clear although there is good evidence for the formation of Au–C bonds [11, 28, 30, 32]. The Au–C bonds formed via electrochemical reduction of aryldiazonium salts are more stable than those obtained by chemisorption of alkanethiols regarding long-term storage and are more resistant to withstand repeated cycling [31, 45]. The modification of Au surface by diazonium reduction is different from that of carbon materials as the reduction peaks also depend on the crystallographic properties of the substrate. Benedetto et al. explained the formation of multi-peaks in cyclic voltammograms during Au modification by the reduction of diazonium salts on different crystallographic sites of gold electrodes [35].

Spontaneous modification of gold surfaces at open circuit potential (OCP) in acetonitrile and aqueous acidic solutions of diazonium salts has been reported in several works [55, 56]. Films prepared at OCP show growth behaviour and composition that are very similar to those

electrografted from acetonitrile solution, except that they suffer from low stability to sonication [56]. Podvorica et al. reported spontaneous chemical and electrochemical grafting of diazotate salts to gold and a successful modification of Au surface with nitrophenyl and bromophenyl groups was achieved [57]. The diazonium chemistry can be used to attach alkylphenyl monolayers to gold nanoparticles [58].

The barrier properties of aryl-modified Au electrodes are of considerable interest from the point of view of basic research. These aspects are also highly relevant for the application of the modified electrodes in electrochemical sensing. Various modifiers have been attached to gold surfaces in order to study their blocking action towards solution-based redox probes. Carboxyphenyl (CP) films efficiently block the Au electrode surface for the electron transfer of the $Fe(CN)_6^{3-/4-}$ redox couple [31]. Even rather porous CP films strongly inhibit this redox process due to the electrostatic repulsion between the negatively charged modifier and anionic redox species [32]. Paulik et al. reported that the blocking behaviour also depends on the environment in which the modifier films have been treated before electrochemical testing [32]. Liu et al. performed a comparative study of gold and glassy carbon electrodes modified with mixed aryl layers by using in situ generated diazonium compounds [48]. The order of reduction potentials for different substituted aryldiazonium salts on Au electrodes was determined to be as follows 4-carboxyphenyl <4-aminothiophenol <4-phenylenediamine <4-nitrophenyl [48].

Gold electrodes modified with aryl groups could be applied in electroanalytical devices and they provide a good platform for the development of biosensors [8, 37, 41, 43]. The better detection limits for the gold electrodes modified with aryldiazonium salts compared with carbon surfaces is attributed both to the lower capacitance and the superior rate of electron transfer at the gold electrodes [8].

Nitrophenyl (NP)-modified Au electrodes have been frequently employed to study the inhibition of electron transfer processes for various redox systems [19, 27, 28, 45, 50]. The barrier properties of the NP films depend on the structure and thickness of the film, which in turn are influenced by the conditions of their electrochemical deposition and even on post-deposition treatment. Solvent and the treatment procedure used play an important role in this regard [59].

Recently, we have investigated the blocking behaviour of gold electrodes modified with four diazonium compounds [51]. However, to our knowledge, there is no literature on the blocking properties of Au/NP and Au/DP electrodes towards O_2 reduction. The blocking action of self-assembled monolayers (SAMs) on Au for O_2 reduction is well-established [60–63] and it was of special interest to compare the results obtained in the present work with those of Au/SAM.

The purpose of this research was to explore the electrochemical properties of nitrophenyl- and decylphenyl-modified Au electrodes and to study the resulting blocking of electron transfer reactions. It was of particular interest to study the effect of polar and non-polar functionalities (i.e. nitro and alkyl groups) on the blocking action of these aryl films.

Experimental

Electrografting of aryl groups to Au electrodes

4-Nitrobenzenediazonium tetrafluoroborate (NBD) was purchased from Aldrich. 4-Decylbenzenediazonium tetrafluoroborate (DBD) was synthesised according to a published procedure [58]. Briefly, DBD was prepared by the diazotisation of 4-aminodecylbenzene (Aldrich) in fluoroboric acid and sodium nitrite.

A polycrystalline gold disc electrode with a geometric area (A) of 0.196 cm^2 was employed for the electrochemical measurements. The disc was cut from an Au rod (99.99%, 0.5 cm in diameter, Alfa Aesar, UK) and was pressed in a Teflon holder. The electrode was polished before use to a mirror finish with 1.0, 0.3 and 0.05 μm alumina slurries (Buehler) followed by sonication in Milli-Q water (Millipore, Inc.). The polished Au electrodes were electrochemically cleaned in Ar-saturated 0.5 M H_2SO_4 by cycling the potential 50 times at 100 mV s^{-1} between −0.3 and 1.5 V. Sulphuric acid (96%, Suprapur) was supplied by Merck.

After the electrochemical cleaning step, the electrode was rinsed thoroughly with Milli-Q water followed by sonication in acetonitrile for 3 min. Then the electrode was transferred immediately to the modification solution, protecting it by a droplet of acetonitrile to avoid exposure to air. Surface grafting was carried out in acetonitrile (ACN, Riedel–de Haën) containing 0.1 M tetrabutylammonium tetrafluoroborate ($TBABF_4$, Fluka) as base electrolyte. $TBABF_4$ was dried under vacuum at 80 °C for 24 h. The concentration of the aryldiazonium salts was 3 mM. For the electrografting experiments, the reference electrode was placed in a separate compartment in order to avoid the penetration of water into the modification solution and a proper junction was made. Fischer titration was used to determine residual water in the modification solution. The initial water quantity was 116 ppm and it increased by two to three times after the electrografting experiments.

The potential was cycled between 0.5 and −1.0 V for the modification with decylphenyl groups and between 0.6 and −0.25 V for the modification with nitrophenyl groups, and then the electrodes were held at −0.25 V for 5 min followed by sonication in ACN for 5 min. The electrodes modified with 4-nitrophenyl and 4-decylphenyl groups are designated

as Au/NP and Au/DP, respectively. Electrochemical grafting of Au surface with aryl groups by diazonium reduction is shown in Scheme 1.

EQCM studies of 4-nitrophenyl film formation

A Research Quartz Crystal Microbalance (Maxtek) was employed to measure resonance frequency shifts in situ. The microgravimetric studies were carried out in a GC-15 three-electrode glass cell, which included a CHC-15 crystal holder, clamp and stopper (Maxtek). A 5-MHz AT-cut quartz crystal (25.4 mm in diameter) vertically positioned in front of the counter electrode served as the working electrode (polycrystalline Au), both sides of which were coated with Au sputtered on a Ti layer in a keyhole pattern (geometric area in contact with solution=1.37 cm^2; Maxtek). The surface was thoroughly cleaned before electrografting by cycling 30 times in N_2-saturated 0.5 M H_2SO_4 between −0.2 and 1.5 V at 100 mV s^{-1} and, if necessary, changing the solution three times. After this step, the cell and electrodes were washed several times with water followed by rinsing with acetonitrile. The surface modification of the working electrode for electrochemical quartz crystal microbalance (EQCM) measurements was carried out in 0.1 M $NaClO_4$/ACN containing 3 mM of NBD. The reference electrode was separated from the modification solution by a jacket equipped with a sintered glass junction in order to minimise water penetration. $NaClO_4 \times H_2O$ (99%) was supplied by Merck.

The Sauerbrey equation was used assuming that the attached layer of NP is rigid and no viscoelastic changes occur at the electrode/solution interface: $\Delta m = -\Delta f / C_f$ [64], where Δm is the change of mass per unit area in g cm^{-2}; Δf is the resonance frequency shift in Hz and C_f is the sensitivity factor of the crystal in Hz ng^{-1} cm^2 (0.056 Hz ng^{-1} cm^2 in the present case).

Surface characterisation of 4-nitrophenyl films on gold

For the X-ray photoelectron spectroscopy (XPS) studies, gold Arrandee™ specimens (250±50) nm thick gold film deposited on a (2.5±1.5) nm chromium layer on borosilicate glass slides (1.1×1.1 cm^2) were used. The XPS measurements were carried out with a SCIENTA SES-100 spectrometer using an unmonochromated Mg Kα X-ray source (incident energy=1253.6 eV), a take-off angle of 90° and a source power of 300 W. The pressure in the analysis chamber was below 10^{-9} Torr. While collecting the survey scan, the following parameters were used: energy range=1,100–0 eV, pass energy=200 eV, step size=0.5 eV and for the high-resolution scan in the N1s region: energy range=415–380 eV, pass energy=200 eV, step size=0.1 eV.

The surface morphology of nitrophenyl-modified Au (111) electrodes as well as that of the bare gold electrode was studied by atomic force microscopy (AFM) with a CP-II (PSI/Veeco) multimode microscope in intermittent contact mode using a NSG01 series cantilevers (NT-MDT) under ambient conditions. The Gwyddion™ free software (Czech Metrology Institute) was employed for image processing and surface roughness calculations. All images were processed by the first order flattening for background slope removal, and if necessary, the contrast and brightness were adjusted. Monocrystalline Au(111) films, used as a substrate for the AFM measurements, were deposited on mica at elevated temperature using electron beam evaporator VS-17 (Vacuum Service OY). The mica substrates were cleaved just before Au deposition. Prior to each experiment the Au(111) film surface was shortly annealed in H_2 flame. Each AFM image presented is representative of numerous images taken on different locations of the sample.

Electrochemical characterisation of the aryl-modified Au electrodes

The electrochemical studies of polished and aryl-modified Au electrodes were carried out by cyclic voltammetry (CV) in 0.1 M K_2SO_4 containing 1 mM $K_3Fe(CN)_6$ (Aldrich). The solution was saturated with Ar (99.999%, AGA) before measurement and a continuous flow of argon was maintained over the solution during the electrochemical measurements. Oxygen reduction was studied with a rotating disc electrode (RDE) in 0.1 M KOH (BDH, AristaR) solution in Milli-Q water; the solutions were saturated with O_2 (99.999%, AGA). For the RDE experiments, an EDI101 rotator and CTV101 speed control unit (Radiometer, Copenhagen) were employed. The electrode rotation rate (ω) was varied from 360 to 4,600 rpm. The potential was applied with an Autolab potentiostat/galvanostat PGSTAT10 (Eco Chemie BV, The Netherlands) and the experiments were controlled with the General Purpose Electrochemical System software. A Pt foil served as the counter electrode and a saturated calomel electrode (SCE) was used as a reference. All the potentials are referred to

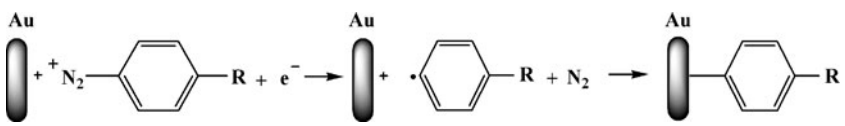

Scheme 1 Electrografting of Au surface with aryl groups by diazonium reduction

this electrode. All experiments were carried out at room temperature (23±1 °C).

Results and discussion

Electrochemical grafting of aryldiazonium cations to Au electrodes

Figure 1 presents electrografting behaviour of aryldiazonium derivatives on a gold electrode with two peaks. The first sharp peak is attributed to the reduction of diazonium cations on Au(111) facets and the second peak observed at more negative potentials corresponds to the reduction on Au(100) domains [35]. The peak potentials for the first cathodic scan were 0.48 and 0.27 V for 4-nitrobenzenediazonium cations (Fig. 1a). These peaks completely disappeared for the second scan caused by the inhibiting effect of the film formed during the first scan. The first electrografting scan of 4-decylbenzenediazonium cations shows a sharp peak at 0.15 V (Fig. 1b), which disappears on consecutive scans. A second peak appears at ca −0.8 V and the current of this peak decreases during repetitive potential cycling. The true origin of this peak is not clear and it is proposed that this could be attributed to the reduction of aryldiazonium cations on Au(110), Au (311) and other crystal faces [35]. However, even after holding the electrode at −0.25 V for 5 min, the residual of this peak is still observed.

Figure 2a shows *I–E* and Δm–*E* potentiodynamic results for an Au electrode during 10 repetitive cycles in 0.1 M $NaClO_4$/ACN containing 3 mM of the 4-nitrobenzenediazonium salt. The current response is similar to that presented in Fig. 1a. The first potential scan shows two current peaks at 0.3 and 0.12 V (see Fig. 2a) corresponding to the reduction of the 4-nitrobenzenediazonium cation. An increase in mass is observed for potentials more negative than 0.53 V, which coincides with the increase of current for the first CV scan. This increase in mass (340 ng cm^{-2}) is linear until around 0.35 V which is very close to the potential of the first reduction peak and the first stage of the attachment of NP groups to the surface of gold film is in evidence. After this potential, in negative potential scan direction, a second increase in mass (150 (=490–340)ng cm^{-2}) with smaller inclination (ng cm^{-2} V^{-1}) is observed until around 0.0 V (second stage of the attachment of NP groups to the surface of gold film). At the end of the first potential half cycle, the increase in mass was 520 ng cm^{-2} and at the end of the first potential cycle was 540 ng cm^{-2}. When the potential scan is reversed, the mass continues to increase slowly. A gradual mass increase is observed on further potential cycling. Comparing the mass change of the first and tenth scans, an increase in mass of approximately 500 ng cm^{-2} is observed for a layer that blocks completely the reduction of the diazonium compound. This behaviour has been previously observed for the covalent grafting of gold with other aryldiazonium compounds [27, 34, 35]. The slow mass increase in the reverse scan has been attributed to the formation of charge–transfer complexes that precipitate on the electrode surface [44, 51, 65] but further growth from the radicals generated and diffusing to the electrode surface cannot be ruled out. The faradaic efficiency was calculated from the slope of the Δm–Δq plots for different experimental conditions and a value of 20% was found for the first electrografting half scan.

By assuming a surface concentration of 10×10^{-10} mol cm^{-2} for a monolayer [27], the corresponding mass expected for a monolayer of NP is 122 ng cm^{-2}. The surface concentration of NP on Au surface can be calculated as 42.6×10^{-10} mol cm^{-2} (520 ng cm^{-2}), indicating significantly higher coverage than a monolayer for the first potential half cycle.

After recording ten consecutive *I–E* and Δm–*E* profiles the electrode was held at a constant potential of −0.25 V for 5 min and a relatively small reduction current was observed during the chronoamperometric experiment (Fig. 2b). Surprisingly, although the current is very small, the mass continues to increase indicating further growth of the grafted layer (i.e. multilayer growth).

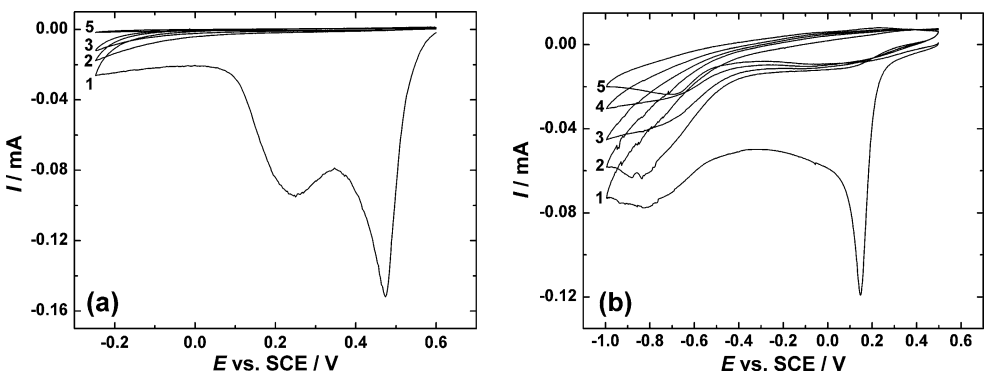

Fig. 1 Electrografting of **a** 4-nitrophenyl and **b** 4-decylphenyl groups to gold in Ar-saturated ACN containing 3 mM of the corresponding aryldiazonium cations and 0.1 M $TBABF_4$ at 100 mV s^{-1}. The first (*1*), second (*2*), third (*3*) and fifth (*4*) potential scans are shown. Curve *5* corresponds to the CV response of an electrode hold at −0.25 V for 5 min

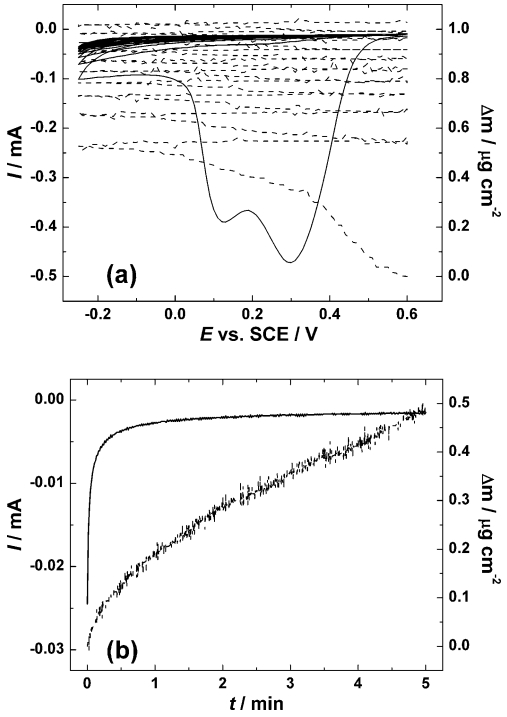

Fig. 2 *I*−*E* (*solid line*) and *Δm*−*E* (*dashed line*) potentiodynamic profiles for ten repetitive potential cycles (**a**) and dynamic profiles for the chronoamperometric experiment (**b**) at −0.25 V for Au electrode in 0.1 M $NaClO_4$/ACN containing 3 mM of 4-nitrobenzenediazonium cations (after 10 potential scans presented)

Surface characterisation of Au/NP electrodes by AFM

Surface morphology of the 4-nitrophenyl-modified gold film on a mica substrate was examined using AFM. Typical topographical images obtained in intermittent contact mode and their height profiles are presented in Fig. 3. It can be seen that bare Au film surface is formed by atomically flat (111) terraces separated by monoatomic steps (see the height profile in Fig. 3a). An atomic resolution STM image of the terrace is also presented (inset to Fig. 3a). These terraces are large enough for detailed topographic studies of NP layers on Au(111) electrodes.

The AFM images of aryl-modified electrodes show clearly that the surfaces of the electrodes are fully covered with granular NP layer (Fig. 3b, c). The granular features of the electrode modified by three potential cycles (Fig. 3b) were uniform with a 15–30 nm average diameter, whereas after 10 voltammetric scans and holding the electrode at −0.25 V, their dimensions varied markedly, with a maximum diameter of 100 nm. It was of considerable interest to determine the characteristic roughness size. Essential increase of the root mean square (RMS) roughness values from 1.9 nm for electrode modified with three voltammetric cycles to 3.2 nm for electrode modified with 10 potential cycles and after holding the same electrode at −0.25 V for 5 min (Fig. 3c), confirms the film roughness and thickness increase with the number of potential cycles. For comparison, the RMS roughness of the unmodified Au(111) surface was 0.2 nm.

XPS analysis of Au/NP electrodes

Figure 4a presents the XPS survey spectrum of 4-nitrophenyl-modified gold electrode grafted by 10 cycles between 0.6 and −0.25 V, followed by holding the electrode at −0.25 V for 5 min. A large decrease of the Au4f peak was observed upon surface modification with NP groups,

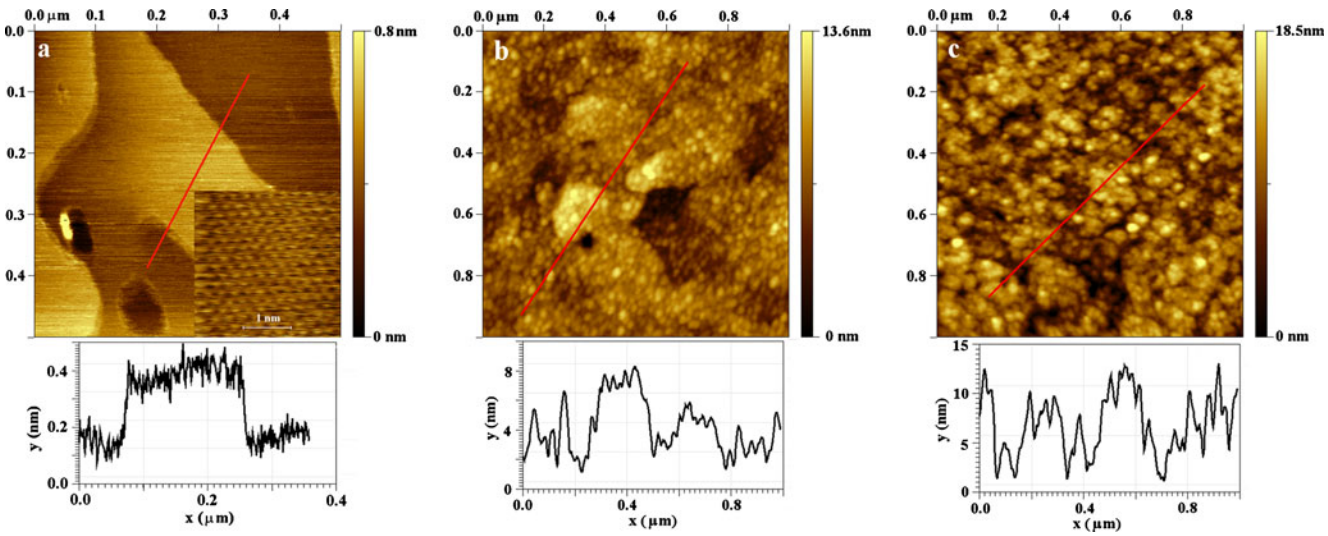

Fig. 3 Typical AFM images and cross-section profiles for a bare gold substrate (**a**), thin Au/NP film (**b**) and thick Au/NP film (**c**). Inset to (**a**) shows an atomic resolution STM image of a similarly pre-treated Au (111) electrode (raw image, 3×3 nm^2). Au electrodes were modified in 0.1 M $TBABF_4$/ACN containing 3 mM 4-nitrobenzenediazonium cations by applying three potential cycles between 0.6 and −0.25 V (**b**) and ten cycles between 0.6 and −0.25 V, followed by holding the electrode at −0.25 V for 5 min (**c**)

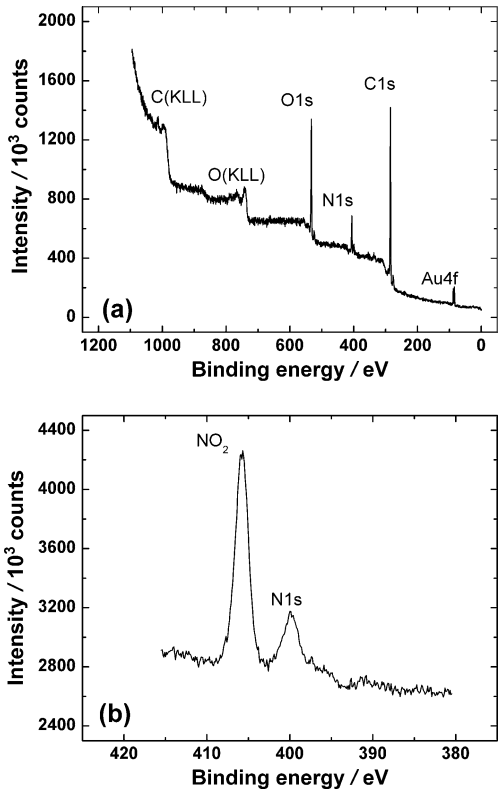

Fig. 4 **a** XPS survey spectrum of a nitrophenyl-modified gold, **b** XPS spectrum of N1s region of nitrophenyl-modified gold. Au electrodes were modified in 0.1 M $TBABF_4$/ACN containing 3 mM 4-nitrobenzenediazonium cations by applying ten potential cycles between 0.6 and −0.25 V, followed by holding the electrode at −0.25 V for 5 min

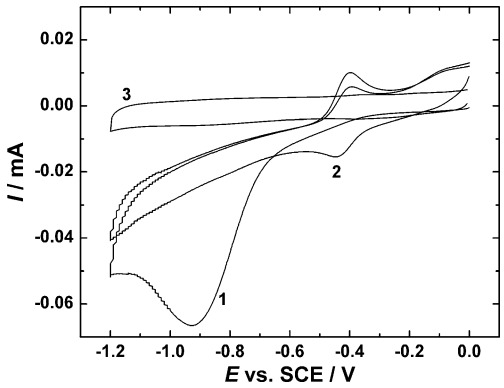

Fig. 5 Cyclic voltammetric response of an Au/NP electrode in Ar saturated 0.1 M KOH at 100 mV s^{-1}. First scan (*1*) and second scan (*2*). Curve *3* corresponds to the cyclic voltammogram of an unmodified Au electrode

although it was still visible. The latter can be explained either due to the formation of a non-uniform thin film or the presence of defect sites. Carbon (C1s) and oxygen (O1s) and, most importantly, the N1s peaks confirm the presence of nitrophenyl groups on the surface. On an unmodified gold surface survey spectra, the N1s peak is totally absent (data not shown). The peak with the binding energy close to 406 eV is attributed to $-NO_2$ functionality, whereas the peak with the binding energy around 400 eV is attributed to amines. It has been demonstrated that X-ray beam during the XPS experiment can chemically transform NO_2 groups to NH_2 groups [66, 67]. Alternatively, the XPS peak at 400 eV can be explained by the presence of azo-linkages (−N=N−) within the NP film [27]. The latter one is more reasonable.

Cyclic voltammetry of Au/NP electrodes

Figure 5 shows repetitive cyclic voltammograms of an Au/NP electrode in Ar-saturated 0.1 M KOH and a typical CV response of bare Au is given for comparison. The first scan shows the irreversible reduction (E_p=−0.93 V) of the NP group to aminophenyl (reaction 1) and hydroxyaminophenyl groups (reaction 2) and on the return scan, oxidation (E_p=−0.4 V) of hydroxyaminophenyl to nitrosophenyl groups (reaction 3) [68]. On the second cycle, the only significant feature is the nitrosophenyl/hydroxyaminophenyl redox couple. This provides further evidence that the gold electrode surface has been modified with NP groups.

$$Ph–NO_2 + 6H^+ + 6e^- \rightarrow Ph–NH_2 + 2H_2O \quad (1)$$

$$Ph–NO_2 + 4H^+ + 4e^- \rightarrow Ph–NHOH + H_2O \quad (2)$$

$$Ph–NHOH \rightleftharpoons Ph–NO + 2H^+ + 2e^- \quad (3)$$

Oxygen reduction on aryl-modified Au electrodes

The oxygen reduction behaviour of aryl-modified gold electrodes was studied in 0.1 M KOH using the RDE method and Fig. 6 shows the representative RDE results. The attachment of 4-nitrophenyl groups (Fig. 6a) and 4-decylphenyl groups (Fig. 6b) to the Au electrode surface inhibits the electrochemical reduction of oxygen. It is well-known that on bare gold in the range of potentials studied, the number of electrons transferred per O_2 molecule is higher than two [69] indicating the further reduction of the peroxide intermediate formed [69].

The electrochemical reduction of oxygen is strongly influenced by the presence of the modifier film (Fig. 6). The half-wave potential of O_2 reduction shifts to negative direction as compared to that of a polished Au electrode. A typical feature of O_2 reduction on polycrystalline gold in alkaline solution is the presence of reduction current peak at ca −0.3 V. Both Au/NP and Au/DP electrodes show

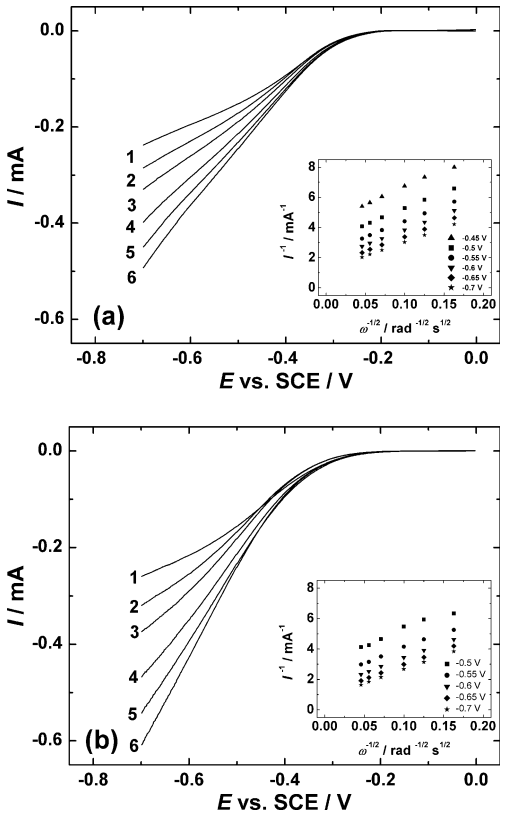

Fig. 6 RDE voltammetry curves for oxygen reduction on **a** Au/NP and **b** Au/DP electrodes at different rotation rates: (*1*) 360, (*2*) 610, (*3*) 960, (*4*) 1,900, (*5*) 3,100 and (*6*) 4,600 rpm in O_2 saturated 0.1 M KOH. ν=20 mV s^{-1}. The insets show the Koutecky–Levich plots for oxygen reduction on modified Au electrodes

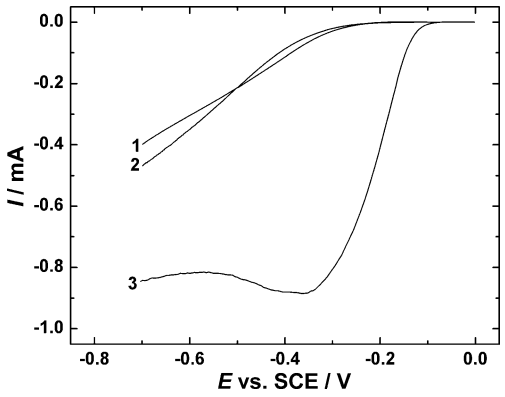

Fig. 7 A comparison of current–potential curves for oxygen reduction on (*1*) Au/NP, (*2*) Au/DP and (*3*) bare Au electrodes at ω=1,900 rpm, ν=20 mV s^{-1}

negligible reduction current at this potential. At more negative potentials, the rate of O_2 reduction increases and current is dependent on the electrode rotation rate (Fig. 6a, b). Obviously, some parts of the catalytically active sites of the underlying gold electrode are not blocked and the reduction of O_2 occurs on these sites. An alternative explanation is the electron tunnelling through aryl films as shown by Yang and McCreery [70]. A comparison of the RDE results on O_2 reduction of 4-nitrophenyl and 4-decylphenyl-modified gold electrodes is presented in Fig. 7. Both modified electrodes have comparable behaviour and are similar to those observed for Au electrodes modified with bromophenyl groups in our previous investigation [51]. It was expected that the behaviour of NP and DP films towards oxygen reduction is different due to the difference in the polarities.

The Koutecky–Levich (K–L) analysis (dependence of $I^{-1/2}$ on $\omega^{-1/2}$) is shown in the insets of Fig. 6a, b. It is evident that the reduction of O_2 is under the mixed kinetic-diffusion control over the entire range of potential studied, since there is a clear intercept of the K–L plots at infinite rotation rate. The non-zero intercept for both modified electrodes gives further evidence for surface blocking and indicates that there are only a limited number of surface sites for oxygen reduction to occur. The number of electrons transferred per O_2 molecule (n) was calculated from these plots using the K–L equation [71]:

$$\frac{1}{I} = \frac{1}{I_k} + \frac{1}{I_d} = -\frac{1}{nFAkC_{O_2}} - \frac{1}{0.62nFAD_{O_2}^{2/3}\nu^{-1/6}C_{O_2}\omega^{1/2}} \quad (4)$$

where I is the measured current, I_k and I_d are the kinetic and diffusion-limited currents, respectively, k is the electrochemical rate constant for O_2 reduction, F is the Faraday constant (96,485 C mol^{-1}), A is the electrode area, ω is the rotation rate, C_{O_2} is the concentration of oxygen in the bulk (1.2×10^{-6} mol cm^{-3} [72]), D_{O_2} is the diffusion coefficient of oxygen (1.9×10^{-5} cm^2 s^{-1} [72]), and ν is the kinematic viscosity of the solution (0.01 cm^2 s^{-1} [73]).

The value of n was close to two for both modified electrodes studied, indicating that the process of O_2 reduction on these electrodes yields hydrogen peroxide as the final product. The results obtained in the present work are consistent with a recent report on oxygen reduction on DP-modified Au nanoparticles [74]. Such behaviour was explained by the hydrophobic local environment created by organic films that stabilise peroxide and superoxide species formed during the reduction of oxygen [74]. A similar conclusion can be made for the present case.

Previous work has shown that O_2 reduction was not completely suppressed even on glassy carbon electrodes modified with various aryl groups [70, 75, 76]. It should be mentioned that the modifier films on glassy carbon are more densely packed than those on gold surface. Therefore, the aryl films studied do not possess excellent barrier properties for O_2 reduction.

It is of considerable interest to compare the blocking effect of aryl films prepared by diazonium reduction with

that of adsorbed thiols (Au/SAM). There are only a few reports on the blocking action of Au/SAMs towards oxygen reduction [60–63]. An early work by Vago et al. showed a strong inhibition of the oxygen reduction kinetics, because of the formation of the ordered densely packed alkanethiol films [62]. The onset potential of oxygen reduction on octadecanethiol-modified Au electrode shifted negative by 0.5 V as compared to that of bare Au. However, after holding the electrode at −0.8 V (vs. SHE) the blocking properties of the film against electron transfer reactions were lost. This is likely due to the reductive desorption of SAMs from the surface of gold. The approach of reductive desorption of SAMs has been employed to tailor-design the modified Au electrodes of desired electrochemical properties. For instance El Deab and Ohsaka observed a quasi-reversible two-electron reduction of O_2 to HO_2^- on gold electrodes modified with a self-assembled submonolayer of cysteine [60].

A recent study by Muglali et al. presents the best comparison with our work because of the application of various pyridine-terminated SAMs on Au(111) [63]. As expected, the blocking behaviour of the adsorbed layers depends primarily on the presence of defects (pinholes) within the film. For SAMs on gold, the inhibition of the O_2 reduction rate increased with increasing the duration of immersion of Au electrodes in the ethanolic solution of pyridinethiols. For small immersion times, large uncovered areas remained on the substrate surface and as a result only a slight negative shift of the O_2 reduction wave was observed. The extent of inhibition was influenced by the structure of the modifier molecule [63]. After long-time immersion, the SAMs on Au suppressed the process of oxygen reduction more efficiently. This was due to the formation of a more compact layer. The number of defects appears to depend on the film structure. The aryl films studied in our work are of different composition and structure. Consequently, these films possess different electrochemical properties. A detailed study is needed to compare the O_2 reduction behaviour of Au electrodes modified with aryl groups by diazonium reduction and self-assembly. This is outside the scope of the present research.

Electrochemical response of the $Fe(CN)_6^{3-}$ probe on modified Au electrodes

The blocking properties of the NP and DP films towards the $Fe(CN)_6^{3-}$ redox probe were studied to further investigate the effect of film structure on the electrochemical behaviour of aryl modified Au electrodes. The CV response of the $Fe(CN)_6^{3-}$ probe is significantly suppressed on Au/DP electrode (Fig. 8, curve 2) and totally suppressed on Au/NP electrode (Fig. 8, curve 1), indicating that the electron transfer rate is much slower for the Au/NP electrode.

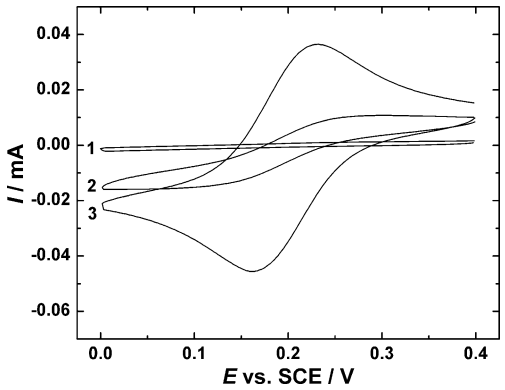

Fig. 8 Cyclic voltammograms recorded in Ar-saturated 0.1 M K_2SO_4 containing 1 mM $K_3Fe(CN)_6$ for (*1*) Au/NP, (*2*) Au/DP and (*3*) bare gold electrodes at 100 mV s^{-1}

Apparently, for the Au/DP electrode there are pinholes or defects in the modifier film and therefore a sigmoidal shape of CVs is observed. For comparison, the electrochemical response of a bare gold electrode is also shown (Fig. 8, curve 3). A pair of well-defined peaks is observed, with a peak to peak separation (ΔE_p) of 65 mV confirming the well-known fast one-electron transfer kinetics for this couple, close to the theoretical value of 60 mV expected for a reversible one-electron transfer process. In our earlier study, we have demonstrated that grafting the Au electrodes with 1- and 2-naphthyl, biphenyl and 4-bromophenyl groups yielded strongly attached layers with high blocking efficiency for the $Fe(CN)_6^{3-/4-}$ redox couple [51]. Recently, the barrier effect of 4-sulfophenyl layer on gold towards the $Fe(CN)_6^{3-}$ redox probe has been studied and it was concluded that the modifier film on Au is not as closely packed as on glassy carbon [49]. Obviously, the higher the surface concentration of the aryl groups, the stronger is the suppression of the electron transfer processes on aryl-modified electrodes. This has been recently demonstrated using surface-bound anthraquinone [77], for which the surface concentration can be easily determined.

An interesting comparison between the barrier properties of thiol-derived and diazonium-derived aryl films on gold towards the $Fe(CN)_6^{3-}$ probe has been made in references [31, 45]. The stability of NP films under various treatments was investigated and the effect of treatment on their electrochemical response was explored. The as prepared NP film completely blocked electron transfer for $Fe(CN)_6^{3-}$ [45]. The CV response revealed poorer barrier properties after refluxing or sonicating in acetonitrile. Apparently, a part of material is removed from the film during these treatments. An enhanced stability of diazonium derived film was in evidence, which is advantageous for the practical application of Au/NP electrodes [45]. Similar observation was made by Liu et al. when studying the stability of carboxyphenyl and mercaptobenzoic acid layers

on Au [31]. The superiority of Au electrodes modified by diazonium reduction over their alkanethiol-derived counterparts for electrochemical sensing applications has been highlighted in a recent review by Gooding [8].

Conclusions

A comprehensive study to investigate the blocking properties of NP and DP films after electrografting to Au surfaces towards O_2 reduction and the $Fe(CN)_6^{3-}$ redox probe has been carried out. The results obtained in this work support strong attachment of aryl groups to Au electrodes via electrochemical grafting of aryldiazonium compounds in acetonitrile. The EQCM results demonstrate that a surface concentration higher than monolayer coverage for the nitrophenyl groups on gold is achieved after the first modification potential cycle. AFM studies of the film growth revealed that the film does not grow uniformly and a rather granular growth is in evidence, which does not result in compact but rather loosely packed film. This finding is also supported by an XPS study where Au4f peak is clearly seen for the films of high nitrophenyl surface concentration. The electrochemical response of the $Fe(CN)_6^{3-}$ probe was completely suppressed on Au/NP electrodes and less suppressed on Au/DP electrodes, the difference in blocking action could be explained by differences in film compactness which is caused by a higher steric hindrance of decylphenyl groups. The kinetics of O_2 reduction was inhibited to a lesser extent on both modified electrodes as compared to that of the $Fe(CN)_6^{3-}$ probe.

Acknowledgements This research was supported by the Estonian Science Foundation (grants nos. 7546 and 8666).

References

1. Delamar M, Hitmi R, Pinson J, Savéant J-M (1992) J Am Chem Soc 114:5883–5884
2. Allongue P, Delamar M, Desbat B, Fagebaume O, Hitmi R, Pinson J, Savéant J-M (1997) J Am Chem Soc 119:201–207
3. Liu Y-C, McCreery RL (1995) J Am Chem Soc 117:11254–11259
4. Saby C, Ortiz B, Champagne GY, Bélanger D (1997) Langmuir 13:6805–6813
5. McCreery RL (1999) Electrochemical properties of carbon surfaces. In: Wieckowski A (ed) Interfacial electrochemistry: theory, experiment, and applications. Marcel Dekker, New York, pp 631–647
6. Downard AJ (2000) Electroanalysis 12:1085–1096
7. Pinson J, Podvorica F (2005) Chem Soc Rev 34:429–439
8. Gooding JJ (2008) Electroanalysis 20:573–582
9. Knigge D, Kaur P, Swain G (2007) Recent trends in chemically modified sp^2 and sp^3 bonded carbon electrodes. In: Bard AJ, Stratmann M, Fujihira M, Rubinstein I, Rusling JF (eds) Encyclopedia of electrochemistry, vol 10. Wiley-VCH, Weinheim, pp 236–260
10. McCreery RL (2008) Chem Rev 108:2646–2687
11. Bernard M-C, Chaussé A, Cabet-Deliry E, Chehimi MM, Pinson J, Podvorica F, Vautrin-Ul C (2003) Chem Mater 15:3450–3462
12. Adenier A, Bernard M-C, Chehimi MM, Cabet-Deliry E, Desbat B, Fagebaume O, Pinson J, Podvorica F (2001) J Am Chem Soc 123:4541–4549
13. Chaussé A, Chehimi MM, Karsi N, Pinson J, Podvorica F, Vautrin-Ul C (2002) Chem Mater 14:392–400
14. Stewart MP, Maya F, Kosynkin DV, Dirk SM, Stapleton JJ, McGuiness CL, Allara DL, Tour JM (2004) J Am Chem Soc 126:370–378
15. Hurley BL, McCreery RL (2004) J Electrochem Soc 151:B252–B259
16. Ghilane J, Delamar M, Guilloux-Viry M, Lagrost C, Mangeney C, Hapiot P (2005) Langmuir 21:6422–6429
17. Combellas C, Delamar M, Kanoufi F, Pinson J, Podvorica FI (2005) Chem Mater 17:3968–3975
18. Adenier A, Cabet-Deliry E, Chaussé A, Griveau S, Mercier F, Pinson J, Vautrin-Ul C (2005) Chem Mater 17:491–501
19. Adenier A, Combellas C, Kanoufi F, Pinson J, Podvorica FI (2006) Chem Mater 18:2021–2029
20. Chamoulaud G, Bélanger DJ (2007) J Phys Chem C 111:7501–7507
21. Kullapere M, Tammeveski K (2007) Electrochem Commun 9:1196–1201
22. Kullapere M, Matisen L, Saar A, Sammelselg V, Tammeveski K (2007) Electrochem Commun 9:2412–2417
23. Janin M, Ghilane J, Randriamahazaka H, Lacroix J-C (2009) Electrochem Commun 11:647–650
24. Isbir-Turan AA, Üstündag Z, Solak AO, Kilic E, Avseven A (2009) Thin Solid Films 517:2871–2877
25. Hinge M, Ceccato M, Kingshott P, Besenbacher F, Pedersen SU, Daasbjerg K (2009) New J Chem 33:2405–2416
26. Ahlberg E, Helgée B, Parker VD (1980) Acta Chem Scand B 34:181–186
27. Laforgue A, Addou T, Bélanger D (2005) Langmuir 21:6855–6865
28. Lyskawa J, Bélanger D (2006) Chem Mater 18:4755–4763
29. Ricci A, Bonazzola C, Calvo EJ (2006) Phys Chem Chem Phys 8:4297–4299
30. Liu G, Liu J, Böcking T, Eggers PK, Gooding JJ (2005) Chem Phys 319:136–146
31. Liu G, Böcking T, Gooding JJ (2007) J Electroanal Chem 600:335–344
32. Paulik MG, Brooksby PA, Abell AD, Downard AJ (2007) J Phys Chem C 111:7808–7815
33. Griveau S, Mercier F, Vautrin-Ul C, Chaussé A (2007) Electrochem Commun 9:2768–2773
34. Haccoun J, Vautrin-Ul C, Chaussé A, Adenier A (2008) Prog Org Coat 63:18–24
35. Benedetto A, Balog M, Viel P, Le Derf F, Sallé M, Palacin S (2008) Electrochim Acta 53:7117–7122
36. Alamarguy D, Benedetto A, Balog M, Noël S, Viel P, Le Derf F, Houzé F, Sallé M, Palacin S (2008) Surf Interface Anal 40:802–805
37. Harper JC, Polsky R, Dirk SM, Wheeler DR, Brozik SM (2007) Electroanalysis 19:1268–1274
38. Harper JC, Polsky R, Wheeler DR, Brozik SM (2008) Langmuir 24:2206–2211
39. Harper JC, Polsky R, Wheeler DR, Lopez DM, Arango DC, Brozik SM (2009) Langmuir 25:3282–3288
40. Polsky R, Harper JC, Wheeler DR, Brozik SM (2008) Electroanalysis 20:671–679
41. Radi A-E, Lates V, Marty J-L (2008) Electroanalysis 20:2557–2562
42. Radi A-E, Muños-Berbel X, Cortina-Puig M, Marty J-L (2009) Electrochim Acta 54:2180–2184

43. Radi A-E, Muños-Berbel X, Cortina-Puig M, Marty J-L (2009) Electroanalysis 21:696–700
44. Kullapere M, Marandi M, Sammelselg V, Menezes HA, Maia G, Tammeveski K (2009) Electrochem Commun 11:405–408
45. Shewchuk DM, McDermott MT (2009) Langmuir 25:4556–4563
46. Boland S, Foster K, Leech D (2009) Electrochim Acta 54:1986–1991
47. Gehan H, Fillaud L, Felidj N, Aubard J, Lang P, Chehimi MM, Mangeney C (2010) Langmuir 26:3975–3980
48. Liu G, Chockalingham M, Khor SM, Gui AL, Gooding JJ (2010) Electroanalysis 22:918–926
49. Gui AL, Liu G, Chockalingam M, Le Saux G, Harper JB, Gooding JJ (2010) Electroanalysis 22:1283–1289
50. Gui AL, Liu G, Chockalingam M, Le Saux G, Luais E, Harper JB, Gooding JJ (2010) Electroanalysis 22:1824–1830
51. Kullapere M, Kozlova J, Matisen L, Sammelselg V, Menezes HA, Maia G, Schiffrin DJ, Tammeveski K (2010) J Electroanal Chem 641:90–98
52. Khosroo M, Rostami AA (2010) J Electroanal Chem 647:117–122
53. Zhang X, Sun G, Hinrichs K, Janietz S, Rappich J (2010) Phys Chem Chem Phys 12:12427–12429
54. Zhang X, Sun G, Hovestädt M, Syritski V, Esser N, Volkmer R, Janietz S, Rappich J, Hinrichs K (2010) Electrochem Commun 12:1403–1406
55. Fan F-RF, Yang J, Cai L, Price DW, Dirk SM, Kosynkin DV, Yao Y, Rawlett AM, Tour JM, Bard AJ (2002) J Am Chem Soc 124:5550–5560
56. Lehr J, Williamson BE, Flavel BS, Downard AJ (2009) Langmuir 25:13503–13509
57. Podvorica FI, Kanoufi F, Pinson J, Combellas C (2009) Electrochim Acta 54:2164–2170
58. Mirkhalaf F, Paprotny JJ, Schiffrin DJ (2006) J Am Chem Soc 128:7400–7401
59. Downard AJ (2009) Int J Nanotechnol 6:233–244
60. El Deab MS, Ohsaka T (2003) Electrochem Commun 5:214–219
61. El Deab MS, Ohsaka T (2004) Electrochim Acta 49:2189–2194
62. Vago ER, de Weldige K, Rohwerder M, Stratmann M (1995) Fresenius J Anal Chem 353:316–319
63. Muglali MI, Bashir A, Rohwerder M (2010) Phys Status Solidi A 207:793–800
64. Buttry DA, Ward MD (1992) Chem Rev 92:1355–1379
65. Menezes HA, Maia G (2006) J Electroanal Chem 586:39–48
66. Adenier A, Cabet-Deliry E, Chausse A, Griveau S, Mercier F, Pinson J, Vautrin-Ul C (2005) Chem Mater 17:491–501
67. Mendes P, Belloni M, Ashwort M, Hardy C, Nikitin K, Fitzmaurice D, Critchely K, Evans S, Preece J (2003) Chem Phys Chem 4:884–889
68. Mirkhalaf F, Tammeveski K, Schiffrin DJ (2009) Phys Chem Chem Phys 11:3463–3471
69. Sarapuu A, Nurmik M, Mändar H, Rosental A, Laaksonen T, Kontturi K, Schiffrin DJ, Tammeveski K (2008) J Electroanal Chem 612:78–86
70. Yang H-H, McCreery RL (2000) J Electrochem Soc 147:3420–3428
71. Bard AJ, Faulkner LR (2001) Electrochemical methods, 2nd edn. Wiley, New York
72. Davis RE, Horvath GL, Tobias CW (1967) Electrochim Acta 12:287–297
73. Lide DR (ed) (2001) CRC handbook of chemistry and physics, 82nd edn. CRC Press, Boca Raton, FL
74. Mirkhalaf F, Schiffrin DJ (2010) Langmuir 26:14995–15001
75. Kullapere M, Jürmann G, Tenno TT, Paprotny JJ, Mirkhalaf F, Tammeveski K (2007) J Electroanal Chem 599:183–193
76. Kullapere M, Mirkhalaf F, Tammeveski K (2010) Electrochim Acta 56:166–173
77. Reilson R, Kullapere M, Tammeveski K (2010) Electroanalysis 22:513–518